Mesoporous Silicon Nanostructures by Pulsed Laser Deposition as Li-ion Battery Anodes

E. Biserni[a,c], N. Garino[b], A. Li Bassi[a,c], P. Bruno[a], C. Gerbaldi*[b,d]

[a] Center for Nano Science and Technology @PoliMi, Istituto Italiano di Tecnologia, Milano, Italy
[b] Center for Space Human Robotics @Polito, Istituto Italiano di Tecnologia, Corso Trento, 21, 10129 Torino, Italy
[c] Energy Department, Politecnico di Milano, Italy
[d] GAME Lab, Department of Applied Science and Technology – DISAT, Institute of Chemistry, Politecnico di Torino, Corso Duca degli Abruzzi 2 4J0129 Torino, Italy

* Corresponding author (C. Gerbaldi). Tel.: +39 011 090 4643; fax: +39 011 090 4699. e-mail address: claudio.gerbaldi@polito.it

Silicon is very attractive as active material for Li-ion battery anodes due to its high theoretical capacity, but proper nanostructuring is needed to accommodate the large volume expansion/shrinkage upon reversible cycling. This would overcome the destructuration induced by the lithiation/delithiation processes, often resulting in poor long-term performance. Hereby, novel mesoporous silicon nanostructures are grown at room temperature by Pulsed Laser Deposition (PLD) directly on top of the Cu current collector surface, and their promising electrochemical behaviour demonstrated in lab-scale lithium cells. Depending on the porosity, easily tunable by PLD, initial specific capacities approaching 300 μAh cm^{-2} are obtained with a quasi-stable reversible cycling. Engineering voids at the nanoscale, by direct introduction of specific porosity during growth, opens up the route for the effective use of silicon as lithium battery anode without the need for any binder or conductive additive which would lower the overall energy density.

Introduction

In the last decade, we are dealing with the rapid development of high performing portable electronic devices, such as smart phones and notebook computers which are becoming more and more greedy in terms of energy requirements. This continuously leads to a strong demand for high capacity and high energy density sources of power, and Li-ion batteries (LIB) are recognized as the system of choice. Today's LIBs partially satisfy the present demands, but there is still room for further improvements [1].
As far as the anode material is concerned, commercial graphite shows excellent capacity retention during battery cycling; nevertheless, despite its good cycling stability and low cost, the low theoretical capacity of 372 mAh g^{-1} is clearly insufficient for the huge

demands of the next generation of high energy density electronic devices as well as electric vehicles [2]. To meet the requirements, several elements that can reversibly alloy with lithium were investigated, including Si, Sn, Al, Ge as well as mixed compounds thereof [3-6]. Because of its exceptional theoretical capacity (>4200 mAh g^{-1}), silicon is one of the most promising candidates among these elements to be used as anode material and has recently attracted very much attention. The main limitations to the wide spreading of its application are related to the extremely high volume change (~300 % [7]) that occurs during lithium insertion and extraction, leading to mechanical fragmentation and active material particle pulverization. Nanostructuration, introduction of voids and addition of other active materials having lower capacity (e.g., carbon) are the main routes currently being explored to bypass this problem. The advantages of nanostructuration have been evidenced in recent works [8-10] which demonstrated the existence of a threshold dimension in silicon particles that prevents from crack propagation upon lithiation.

The introduction of pores in the silicon anodes is another well-known strategy to face the detrimental effects of volume variation [11-13]; indeed, depending on their size and distribution, voids can accommodate the expansion during lithiation, mitigate internal stresses and possibly prevent from fragmentation and detachment from the current collector. Porous Si films are generally prepared via electrochemical etching using hydrofluoric acid [14,15] or by electrodeposition [16-18].

In this work, we explore the possibility of growing mesoporous hierarchical amorphous silicon nanostructures by simple and rapid Pulsed laser Deposition (PLD). As it allows to easily tailor the film morphology at the nanoscale, both in terms of nanostructure and introduction of voids, PLD enables a straightforward engineering of the anode material properties. In our silicon anodes we introduce a controlled porosity to buffer the volume expansion; moreover, the preferential growth in the direction perpendicular to the substrate heads to favouring the electronic and ionic transport within the anode. Different films were fabricated having different morphology and degree of porosity and the effect of increasing porosity was studied at ambient temperature by electrochemical testing in lithium cell configuration with liquid electrolyte. The best performing samples allowed for good initial capacity approaching 300 $\mu A\ cm^{-2}$ and improved stability over the initial 30 galvanostatic discharge/charge cycles.

Methods

Material preparation

Silicon films were grown at room temperature by the Pulsed Laser Deposition (PLD) technique. A rotating and translating Si crystalline wafer was ablated by a KrF pulsed laser (248 nm, ~ 5 J cm^{-2}, 20 Hz, target-to-substrate distance 50mm) under controlled atmosphere (mixture of < 3 % vol. H_2 in Ar as background gas) in a vacuum chamber, previously evacuated at 3×10^{-3} Pa. In order to grow films having different morphology and porosity, samples were produced under various background pressures of 40, 60 and 100 Pa, respectively. By increasing the background gas pressure, higher porosity can be introduced in the film by means of inducing the formation of bigger clusters during flight with a lower kinetic energy and, hence, a less-packed film on the substrate. Details on the relationship between process parameters and morphology of the Si films are reported in a previous work [19].

After native oxide removal by means of citric acid, copper discs were used as a substrate for Si deposition, so to act as the current collector for the active anode material in lithium cell.

Material characterization

In order to characterize their morphology and thickness, the cross-sections of the mesoporous Si films were imaged by a Supra 40 Zeiss Field Emission Scanning Electron Microscope (FESEM, accelerating voltage 3-5 kV).

Specific surface area (SSA) was determined on a Quadrasorb evo™ (Quantachrome Instruments) using the Brunauer, Emmett, Teller (BET) method. Prior to adsorption, approximately 100.0 mg of solid were placed in the cell and evacuated at about 50 °C for 2 h and, successively, at 200 °C for 3h.

The electrochemical response in liquid electrolyte of the samples was tested in polypropylene three-electrode T-cells assembled as follows: a Si film disk (area 0.785 cm^2) as the working electrode, a 1.0 M lithium hexafluorophosphate ($LiPF_6$, Solvionic, France, battery grade) in a 1:1 w/w mixture of ethylene carbonate (EC) and dimethyl carbonate (DMC) electrolyte solution soaked on a Whatman® GF/A separator and a lithium metal foil (high purity lithium foils, Chemetall Foote Corporation) as the counter electrode. For cyclic voltammetry (CV), a second lithium foil was added at the third hole of the cell, in direct contact with the electrolyte, acting as the reference electrode.

Galvanostatic discharge/charge cycling (cut off potentials: 0.02 – 1.5 V vs. Li^+/Li) and CVs (between 0.02 and 1.5 V vs. Li^+/Li, at 0.1 mV s^{-1} scan rate) were carried out at ambient temperature on an Arbin Instrument Testing System model BT-2000. Clean electrodes and fresh samples were used for each test. Procedures of cell assembly were performed in the inert atmosphere of a dry glove box (MBraun Labstar, O_2 and H_2O content < 1 ppm) filled with extra pure Ar 6.0.

Experimental

Structural and morphological characterization

In the present work, a very simple single-step process allowed to obtain vertically oriented thin films of mesoporous nanostructured silicon, as evidenced by FESEM analysis for morphological characterisation. The length of the columnar nanostructures was found to be approximately 1 μm, as shown in images (a), (c) and (e) of Figure 1 where the low magnification cross-sectional views of the different amorphous silicon films are depicted.

The fabrication method was chosen and tuned so as to grow hierarchical films featured by aggregation of clusters in a columnar mesoporous algae-like structure (see images b, d, f in Figure 1). This was meant, on the one hand, to introduce some degree of porosity, thus accounting for volume expansion of lithiated silicon and, on the other hand, to address the need for overall mechanical integrity. In addition, the anisotropic, aligned columnar structure could in principle be favourable for promoting fast kinetics and a more effective electronic transport throughout the whole electrode thickness as well as hinder the segregation of particles during electrochemical operation.

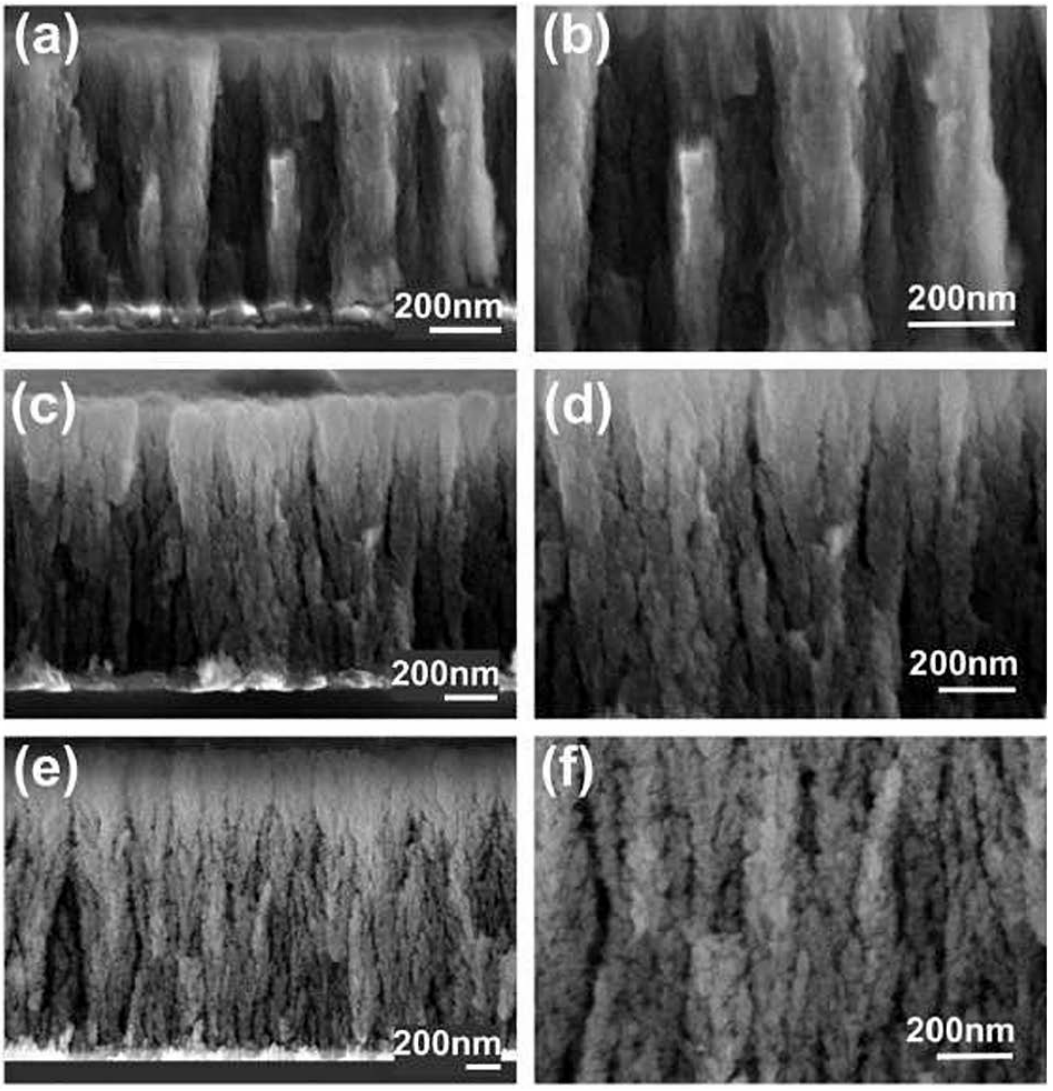

Figure 1 FESEM cross-sectional images showing the different morphology of the mesoporous silicon nanostructured films grown at increasing background gas pressure: (a, b) 40Pa, (c, d) 60Pa, (e, f) 100Pa.

An estimate of the densities of these films is provided in a previous work[19], with a value of 0.36 g cm^{-3} for the sample 100 Pa, 0.92 g cm^{-3} for 60 Pa and 1.66 g cm^{-3} for 40 Pa, which, if compared to the density of 2.33 g cm^{-3} of bulk silicon, result in an estimated porosity of about 85, 60 and 29 %, respectively.

Accurate determination of specific surface area (SSA) in porous Si is usually performed through BET technique that analyses the adsorption/desorption isotherms of gases at low temperature [20]. Nitrogen gas sorption isotherms are shown in Figure 2 (a-c). BET method reveals high surface areas for all of the films and noticeable differences in the position of the hysteresis in isotherm curves, which accounts for different pore size distribution. Exploiting the BET theory, the following values of specific surface area were obtained for each sample prepared varying the deposition pressures: 68 $m^2 g^{-1}$ for sample 40 Pa, 109 $m^2 g^{-1}$ for sample 60 Pa and 189 $m^2 g^{-1}$ for sample 100 Pa.

As expected, surface area values increase almost linearly with the increase in the applied deposition pressure from 40 to 100 Pa, in good agreement with previous literature on porous films prepared by PLD both for silicon or other materials [21,22].

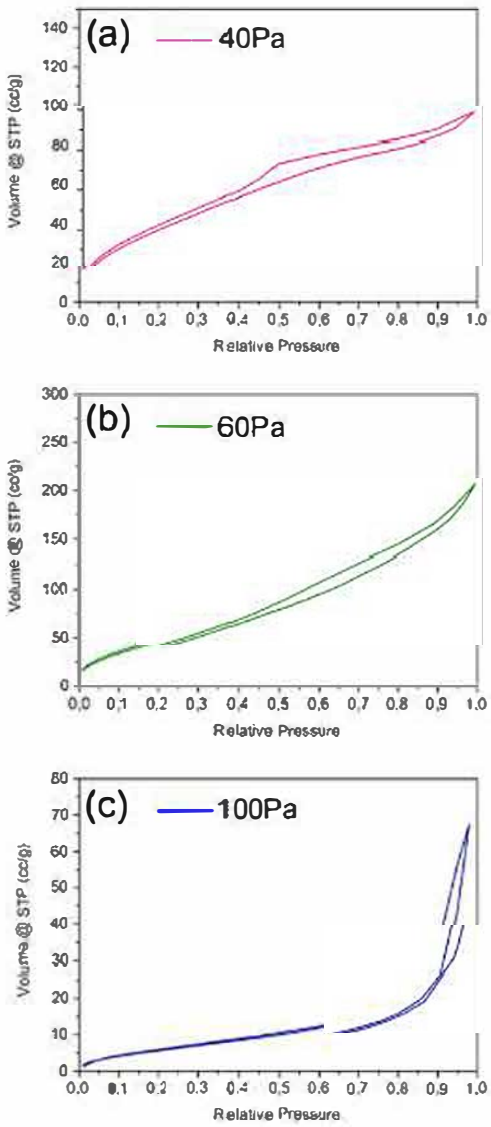

Figure 2 Isothermal profiles of samples prepared at increasingly higher applied deposition pressures: (a) 40Pa, (b) 60Pa, (c) 100Pa.

Electrochemical cell test

The ambient temperature electrochemical behaviour was evaluated in laboratory scale lithium test cells and carried out by means of cyclic voltammetry and galvanostatic discharge/charge cycling at various current regimes. Results are shown in the plots of Figure 3 (a-c). Note that the electrodes were used as-grown on the Cu current collector, without any addition of binders and/or conducting additives.

The typical cyclic voltammetric response of the porous silicon nanostructures prepared by PLD, in particular of sample 40 Pa representative of all of the samples prepared, is shown in Figure 3 (a) in its initial 10 cycles. It was performed at the scan rate of 0.1 mV s^{-1} between 0.02 and 1.5 V vs. Li^+/Li. The cyclic voltammograms (CV) show the characteristic behaviour of silicon electrodes upon reversible alloying/dealloying reactions with lithium ions [23,24], resulting in two main couples of anodic and cathodic peaks. In details, in the initial scan towards lower potential values, it shows two cathodic peaks at below 0.2 V vs. Li^+/Li (i.e., around 0.15 V as the dominant, and around 0.05 V), characteristics of the lithiation step into amorphous silicon. These are reflected in the following anodic scan, where the two corresponding broad anodic peaks, centred at about 0.3 V and 0.47 V vs. Li^+/Li, indicate a two-step lithium extraction process from the Li–Si alloy back to amorphous Si.

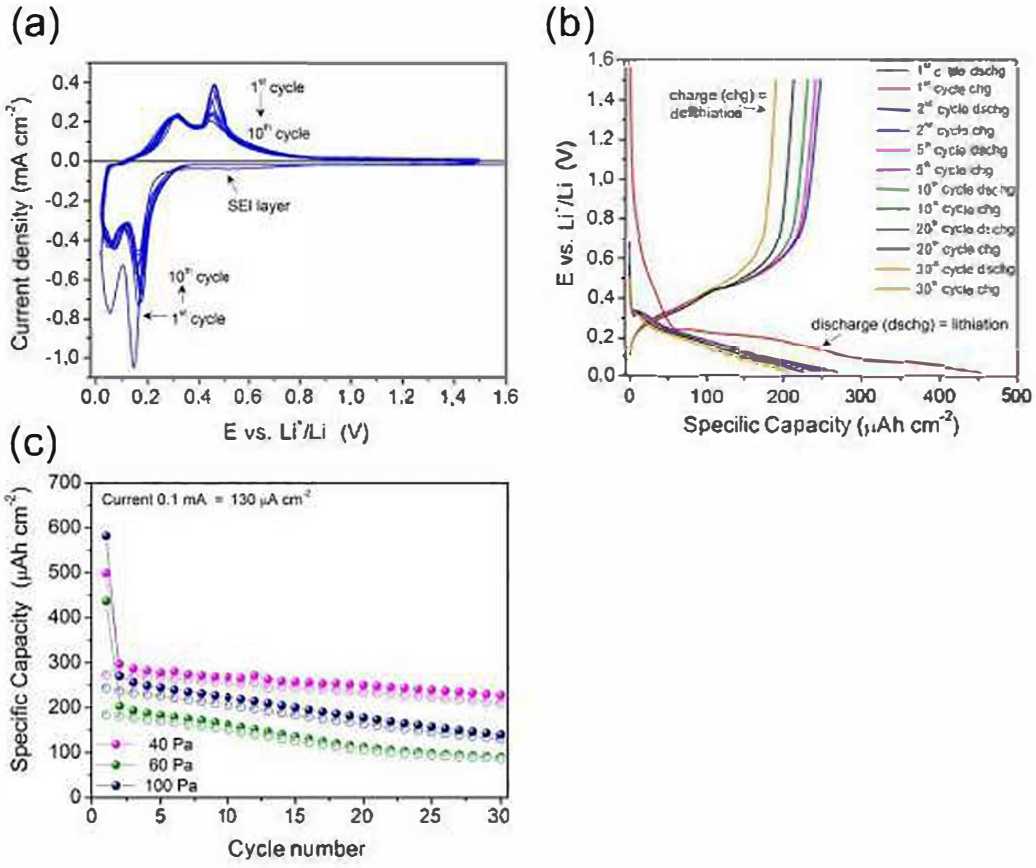

Figure 3 Room temperature electrochemical behaviour in lithium test cells of as-grown mesoporous silicon nanostructures: (a) cyclic voltammetry (cycles 1-10) in the potential range of 0.02–1.5 V vs. Li^+/Li at a scan rate of 0.1 mV s^{-1}, (b) galvanostatic discharge/charge potential vs. specific capacity profiles, (c) specific capacity vs. cycle number.

In the second cathodic scan, the broad cathodic peaks slightly shift towards higher potential values (e.g., the dominant centred at ca. 0.18 V). It is supposed to come from a slightly different kinetics in the alloying process due to the formation of slightly different metastable amorphous Li_xSi phases according to the previous literature [25]. Regarding the

formation of the solid electrolyte interphase (SEI) layer, it appears in the first cathodic scan as a broad faint signal between 0.6 V and 0.4 vs. Li^+/Li.

The discharge (lithiation) and charge (delithiation) potential vs. time profiles for sample 40 Pa, representative for all the samples prepared, are plotted in Figure 3 (b). The charge/discharge current rate used for each sample was 0.1 mA, corresponding to about 130 $\mu A\ cm^{-2}$. Profiles show the typical features of amorphous silicon electrodes, with an initial discharge cycle being rather different from the following ones due to the formation of the SEI layer and to the presence of a high oxygen content at the surface of the electrode, as usual for amorphous silicon nanoparticles. This causes the relatively large irreversible capacity loss which results in low initial Coulombic efficiency for these kind of electrode materials.

The cycling performance of porous silicon nanostructures as a lithium battery anode is reported in Figure 3 (c).

The first 30 galvanostatic cycles show a good initial capacity higher than 200 $\mu Ah\ cm^{-2}$ for all of the three porous films, with a capacity loss of around 40 % for sample 40 Pa and 50 % for both 60 Pa and 100 Pa upon initial lithiation; this is a reasonably low value for losses if compared to similar high-surface-area silicon nanostructures reported in the literature [24]. Based on the kind of synthesis adopted in the present work, the sample having lower surface area available for reaction with the electrolyte, i.e. the one prepared at a pressure of 40 Pa, show in fact lower capacity loss during first lithiation. This reflects also in the overall electrochemical behaviour, which is superior both in terms of higher specific capacity values and stability upon reversible cycling, and results in the highest value of capacity retention (around 77 %) after 30 discharge/charge cycles in lithium cell.

Conclusions

Mesoporous silicon anode nanostructures were fabricated by fast and reliable pulsed laser deposition technique, characterised and electrochemically tested in lithium test cells.

Different deposition pressures were applied in order to evaluate the influence of this process parameter on the morphological/electrochemical characteristics of the resulting nanostructures. The sample prepared at lower deposition pressure, having porosity featured by larger average dimension and lower surface area, show good initial capacity approaching 300 $\mu A\ cm^{-2}$ and improved stability over the initial 30 galvanostatic discharge/charge cycles.

We believe that the improved stability in the samples with larger pores can be related to their lower surface area. On the contrary, the higher surface area of the samples with smaller pore dimension (samples 60 Pa and 100 Pa) is likely to be responsible for their increased capacity fade; more surface area is involved, in fact, in the side reactions with the electrolyte and, hence, more capacity is lost in forming the interphase layer.

Summarizing, the focus of this work was to explore the feasibility of using PLD, a facile one-step technique working at ambient conditions, to finely tune the mesoporous nanostructure of silicon anodes. Once this first investigation has been carried out on how the mesoporosity impacts the electrochemical behaviour of our silicon anodes, our future strategies has to address to the improvement of the specific capacity as well as the cycling stability to reach long-term operation.

References

1. Whittingham, M. S. Materials Challenges Facing Electrical Energy Storage. *MRS Bull.* **33,** 411 (2011).

2. Si, Q. *et al.* A high performance silicon/carbon composite anode with carbon nanofiber for lithium-ion batteries. *J. Power Sources* **195,** 1720 (2010).

3. Fister, T. T. *et al.* Lithium Intercalation Behavior in Multilayer Silicon Electrodes. *Adv. Energy Mater.* **4,** 1301494 (2014).

4. Li, W. *et al.* Germanium nanoparticles encapsulated in flexible carbon nanofibers as self-supported electrodes for high performance lithium-ion batteries. *Nanoscale* **6,** 4532 (2014).

5. Goriparti, S. *et al.* Review on recent progress of nanostructured anode materials for Li-ion batteries. *J. Power Sources* **257,** 421 (2014).

6. Liu, Y., Ma, R., He, Y., Gao, M. & Pan, H. Synthesis, Structure Transformation, and Electrochemical Properties of Li 2 MgSi as a Novel Anode for Li-Ion Batteries. *Adv. Funct. Mater.* **24,** 3944 (2014).

7. Obrovac, M. N. & Krause, L. J. Reversible Cycling of Crystalline Silicon Powder. *J. Electrochem. Soc.* **154,** A103 (2007).

8. Lithiation, N. D. *et al.* Size-Dependent Fracture of Silicon. 1522 (2012).

9. Kalnaus, S., Rhodes, K. & Daniel, C. A study of lithium ion intercalation induced fracture of silicon particles used as anode material in Li-ion battery. *J. Power Sources* **196,** 8116 (2011).

10. Szczech, J. R. & Jin, S. Nanostructured silicon for high capacity lithium battery anodes. *Energy Environ. Sci.* **4,** 56 (2011).

11. Gowda, S. R. *et al.* Three-dimensionally engineered porous silicon electrodes for li ion batteries. *Nano Lett.* **12,** 6060 (2012).

12. Wu, H. *et al.* Engineering empty space between Si nanoparticles for lithium-ion battery anodes. *Nano Lett.* **12,** 904 (2012).

13. Zhao, Y., Liu, X., Li, H., Zhai, T. & Zhou, H. Hierarchical micro/nano porous silicon Li-ion battery anodes. *Chem. Commun. (Camb).* **48,** 5079 (2012).

14. De Boor, J. *et al.* Temperature and structure size dependence of the thermal conductivity of porous silicon. *EPL (Europhysics Lett.* **96,** 16001 (2011).

15. Zhu, J., Gladden, C., Liu, N., Cui, Y. & Zhang, X. Nanoporous silicon networks as anodes for lithium ion batteries. *Phys. Chem. Chem. Phys.* **15,** 440 (2013).

16. Martineau, F. *et al.* Electrodeposition at room temperature of amorphous silicon and germanium nanowires in ionic liquid. *IOP Conf. Ser. Mater. Sci. Eng.* **6,** 012012 (2009).

17. Epur, R., Ramanathan, M., Beck, F. R., Manivannan, A. & Kumta, P. N. Electrodeposition of amorphous silicon anode for lithium ion batteries. *Mater. Sci. Eng. B* **177,** 1157 (2012).

18. Gu, J., Fahrenkrug, E. & Maldonado, S. Direct electrodeposition of crystalline silicon at low temperatures. *J. Am. Chem. Soc.* **135,** 1684 (2013).

19. Biserni, E. *et al.* Room temperature fabrication of silicon nanocrystals by pulsed laser deposition. *J. Nanoparticle Res.* **16,** 2461 (2014).

20. Brunauer, S., Emmett, P. H. & Teller, E. Adsorption of Gases in Multimolecular Layers. *J. Am. Chem. Soc.* **60,** 309 (1938).

21. Passoni, L. *et al.* Hyperbranched quasi-1D nanostructures for solid-state dye-sensitized solar cells. *ACS Nano* **7,** 10023 (2013).

22. Casari, C. S. & Li Bassi, A. in *Adv. Laser Opt. Res.* (Arkin, W. T.) **7,** 65 (Nova Science Publishers, Inc., 2012).

23. Kasavajjula, U., Wang, C. & Appleby, A. J. Nano- and bulk-silicon-based insertion anodes for lithium-ion secondary cells. *J. Power Sources* **163,** 1003 (2007).

24. Li, X. *et al.* Mesoporous silicon sponge as an anti-pulverization structure for high-performance lithium-ion battery anodes. *Nat. Commun.* **5,** 1 (2014).

25. Green, M., Fielder, E., Scrosati, B., Wachtler, M. & Moreno, J. S. Structured Silicon Anodes for Lithium Battery Applications. *Electrochem. Solid-State Lett.* **6,** A75 (2003).